



## 1 **Temperature-dependent diffusion coefficient of H<sub>2</sub>SO<sub>4</sub> in air: 2 laboratory measurements using laminar flow technique**

3 David Brus<sup>1, 2</sup>, Lenka Skrabalova<sup>2, 3</sup>, Erik Herrmann<sup>4</sup>, Tinja Olenius<sup>5\*</sup>, Tereza Travnickova<sup>6</sup> and  
4 Joonas Merikanto<sup>1</sup>

5

6 [1] {Finnish Meteorological Institute, Erik Palménin aukio 1, P.O. Box 503, FIN-00100  
7 Helsinki, Finland}

8 [2] {Laboratory of Aerosols Chemistry and Physics, Institute of Chemical Process Fundamentals  
9 Academy of Sciences of the Czech Republic, Rozvojova 135, CZ-165 02 Prague 6, Czech  
10 Republic}

11 [3] {Department of Physical Chemistry, Faculty of Science, Charles University in Prague,  
12 Hlavova 8, Prague, 128 43, Czech Republic}

13 [4] {Laboratory of Atmospheric Chemistry, Paul Scherrer Institute, CH-5232 Villigen PSI,  
14 Switzerland}

15 [5] {Department of Physics, University of Helsinki, Gustaf Hällströmin katu 2 A, P.O. Box 64,  
16 FIN-00014 Helsinki, Finland}

17 \* Current address: Department of Environmental Science and Analytical Chemistry (ACES) and  
18 Bolin Centre for Climate Research, Stockholm University, SE-10691 Stockholm, Sweden}

19 [6] {Department of Multiphase Reactors, Institute of Chemical Process Fundamentals Academy  
20 of Sciences of the Czech Republic, Rozvojova 135, CZ-165 02 Prague 6, Czech Republic}

21 Correspondence to: D.Brus (david.brus@fmi.fi)

22



23 **Abstract**

24 We report measurements of the diffusion coefficient of sulfuric acid in humidified air at a range  
25 of relative humidities (from ~4 to 70 %), temperatures (278, 288 and 298 K) and initial  $\text{H}_2\text{SO}_4$   
26 concentration (from  $1 \times 10^6$  to  $1 \times 10^8$  molec.  $\text{cm}^{-3}$ ). The diffusion coefficients were estimated from  
27 the sulfuric acid wall loss rate coefficients under laminar flow conditions. The flow conditions  
28 were verified with additional fluid dynamics model CFD-FLUENT simulations which also  
29 reproduced the loss rate coefficients very well at all three temperatures with the maximum  
30 difference of 7 % between the measured and simulated values. The concentration of  $\text{H}_2\text{SO}_4$  was  
31 measured continuously with chemical ionization mass spectrometer (CIMS) at seven different  
32 positions along the flow tube. The wall losses of  $\text{H}_2\text{SO}_4$  were determined from the slopes of fits  
33 to measured  $\text{H}_2\text{SO}_4$  concentrations as a function of the position along the flow tube. The  
34 observed wall loss rate coefficients, and hence the diffusion coefficients, were independent of  
35 different initial  $\text{H}_2\text{SO}_4$  concentrations and different total flow rates. However, the determined  
36 diffusion coefficients decreased with increasing relative humidity, as also seen in previous  
37 experiments, and had a rather strong power dependence of the diffusion coefficient with respect  
38 to temperature, around  $\propto T^{5.4}$ , which is in disagreement with the expected temperature  
39 dependency of  $\sim T^{1.75}$  observed for other gases and not tested before for sulfuric acid. The effect  
40 of relative humidity on the diffusion coefficient is likely due to stronger hydration of  $\text{H}_2\text{SO}_4$   
41 molecules and likely also due to the presence of trace impurities such as amines, possibly  
42 brought to the system by humidification. Clustering kinetics simulations using quantum chemical  
43 data suggest that also the strong temperature dependence of the observed diffusion coefficient  
44 might be explained by increased diffusion volume of  $\text{H}_2\text{SO}_4$  molecules due to stronger clustering  
45 with base-impurities like amines.

46 **1. Introduction**

47 Sulfate aerosols play a dominant role in atmospheric chemistry and have undoubtedly influence  
48 on humans' health and Earth's climate. Gas phase sulfuric acid is formed via oxidation reaction  
49 of  $\text{SO}_2$  with  $\text{OH}$  radicals. The loss of gaseous  $\text{H}_2\text{SO}_4$  in the atmosphere is caused by new particle  
50 formation events, acid-base reactions and cluster formation, and condensation on pre-existing  
51 atmospheric particles. The growth of a particle is driven by condensation of surrounding vapour  
52 on its surface, and the diffusion coefficient ( $D$ ) of  $\text{H}_2\text{SO}_4$  is often used in mass transport  
53 calculations in aerosol chemistry and physics. Condensation and evaporation rates are key  
54 parameters in aerosol dynamics models, and the accuracy of these rates is highly dependent on



55 the values used for the binary diffusion coefficients (Seinfeld and Pandis, 1998). Under certain  
56 circumstances, the gas phase diffusion can even limit the overall rates of condensation and  
57 reactions of trace gases with aerosol particles via influencing the uptake of gas molecules onto  
58 the surface (Tang et al., 2014). The factor that determines if a  $\text{H}_2\text{SO}_4$  molecule will attach to pre-  
59 existing aerosol or stay in the gas phase, possibly contributing to subsequent new particle  
60 formation, is the mass accommodation coefficient (Pöschl et al., 1998). Together with  
61 information on the mass accommodation coefficient, detailed knowledge on the diffusion  
62 coefficient is necessary for accurately simulating atmospheric condensation processes.

63 In this paper we report laboratory measurements of the diffusion coefficient of sulfuric acid in  
64 air. The diffusion coefficient of  $\text{H}_2\text{SO}_4$  was estimated from the first order rate coefficients of the  
65 wall losses of  $\text{H}_2\text{SO}_4$  in a flow tube. The measurements were conducted at atmospheric pressure  
66 under different experimental conditions in order to assess the effect of temperature, relative  
67 humidity, residence time and initial  $\text{H}_2\text{SO}_4$  concentration on the diffusion coefficient of  $\text{H}_2\text{SO}_4$ .

68 All previous measurements of the sulfuric acid diffusion coefficient have been carried out using  
69 nitrogen as the carrier gas and a laminar flow technique. Pöschl et al. (1998) studied the gas-  
70 phase diffusion of  $\text{H}_2\text{SO}_4$  at  $T=303$  K, Lovejoy and Hanson (1996) performed experiments at  
71  $T=295$  K, and Hanson and Eisele (2000) at  $T=298$  K. To our best knowledge, we here present the  
72 first study that investigates systematically the temperature dependency of the diffusion  
73 coefficient of  $\text{H}_2\text{SO}_4$ . In a previous study (Hanson and Eisele, 2000) the RH dependency of  
74  $\text{H}_2\text{SO}_4$  diffusion was investigated, but results reporting the temperature dependency have not  
75 been published before.

76 The Chapman-Enskog theory on gas kinetics predicts the binary diffusion coefficient to depend  
77 on the temperature as  $D \propto T^{1.5}$  when approximating the gas molecules as hard spheres. Fuller et  
78 al. (1966) used a semi-empirical method based on the best nonlinear least square fit for a  
79 compilation of 340 experimental diffusion coefficients, and obtained a temperature dependence  
80 of  $T^{1.75}$ . The Fuller et al. method is known to yield the smallest average error, hence it is still  
81 recommended for use (Reid et al., 1987). According to a compilation work of Marrero and  
82 Mason (1972), the temperature dependence of diffusion coefficients in binary gas mixtures in  
83 most cases varies between  $T^{1.5}$  and  $T^2$ . However, gaseous sulfuric acid vapour can undergo strong  
84 clustering due to presence of base impurities, as noted in several previous experiments (e.g.  
85 Petäjä et al 2011; Almeida et al., 2013; Neitola et al. 2015, Rondo et al. 2016). Such base  
86 impurities are unavoidably present also in our experiment, and most probably they originate



87 from the humidification of the carrier gas (e.g. Benson et al., 2011; Kirkby et al., 2011; Neitola  
88 et al. 2015). Cluster kinetic simulations have suggested that the diffusion coefficient of sulfuric  
89 acid is likely sensitive to such clustering (Olenius et al., 2014), which on the other hand is  
90 sensitive to temperature. Here, we use several approaches to verify the experimental method, and  
91 examine our results against the predictions of the semi-empirical formula as well as data from  
92 the previous experiments. In addition, we assess the effect of molecular cluster formation by  
93 cluster kinetics simulations with quantum chemical input data.

94 **2. Methods**

95 The experimental setup used in this study was described in detail in our previous work (Neitola  
96 et al., 2014; Skrabalova et al., 2014) and therefore only a brief description is given here. The  
97 whole experimental apparatus consists of four main parts: a saturator, a mixing unit, a flow tube  
98 and the sulfuric acid detection system – Chemical Ionization Mass Spectrometer (CIMS) (Eisele  
99 and Tanner, 1999), presented in Figure 1. The  $\text{H}_2\text{SO}_4$  wall loss measurements were carried out in  
100 a laminar flow tube at three temperatures of  $278.20(\pm 0.2)$ ,  $288.79(\pm 0.2)$ , and  $298.2(\pm 0.2)$  K  
101 using purified, particle free and dry air as a carrier gas. The flow tube is a vertically mounted  
102 cylindrical tube made of stainless steel with an inner diameter (I.D.) of 6 cm and a total length of  
103 200 cm. The whole flow tube was insulated and kept at a constant temperature with two liquid  
104 circulating baths (Lauda RK-20). The flow tube consists of two 1 meter long parts; one of them  
105 is equipped with 4 holes in the distance of 20 cm from each other, see Figure 1. Sulfuric acid  
106 vapour was produced by passing a stream of carrier gas through a saturator filled with 95-97 %  
107 wt. sulfuric acid (J.T. Baker analysed). As a saturator we used a horizontal iron cylinder with  
108 Teflon insert (I.D. 5 cm) and it was thermally controlled using a liquid circulating bath (LAUDA  
109 RC-6). The temperature inside the saturator was measured with a PT100 thermocouple ( $\pm 0.05$   
110 K). The carrier gas saturated with  $\text{H}_2\text{SO}_4$  was then introduced with a flow rate from 0.1 to 1 l  
111  $\text{min}^{-1}$  into the mixing unit made of Teflon and turbulently mixed with a stream of humidified  
112 particle free air. The gas mixture was then introduced into the flow tube. The flow rate of the  
113 mixing air varied in most of the experiments from about 7 to 10 l  $\text{min}^{-1}$ . The mixing air was  
114 humidified with one pair of Nafion humidifiers (Perma Pure MH-110-12) connected in parallel,  
115 where the flow of the mixing air was split into half for longer residence time and better  
116 humidification in both humidifiers. Ultrapure water (Millipore, TOC less than 10 ppb, resistivity  
117  $18.2 \text{ M}\Omega\text{cm } @25^\circ\text{C}$ ) circulating in both humidifiers was temperature controlled with liquid  
118 circulating bath (Lauda RC-6 CS). The mixing unit was kept at room temperature and it was not



119 insulated. The mixing unit had following dimensions: O.D. = 10 cm, I.D. = 7 cm and height = 6  
120 cm. Both lines of the carrier gas (saturator and mixing air) were controlled by a mass flow  
121 controller to within  $\pm 3\%$  (MKS type 250). The relative humidity was measured at the centre and  
122 far end of the flow tube with two humidity and temperature probes (Vaisala HMP37E and  
123 humidity data processor Vaisala HMI38) within accuracy of  $\pm 3\%$ .  
124 The sulfuric acid diffusion coefficients were estimated as a function of relative humidity from  
125 the  $\text{H}_2\text{SO}_4$  loss measured by CIMS along the flow tube. The detailed information regarding the  
126 operational principles and calibration of CIMS is given in Eisele and Tanner, (1993); Mauldin et  
127 al., (1998) and Petäjä et al., (2009) and therefore will not be given here again. The charging and  
128 detection efficiency of CIMS in the presence of trace concentrations of base impurities is  
129 discussed thoroughly theoretically (e.g. Kupiainen-Määttä et al., 2013; Ortega et al., 2014) and  
130 also in recent experimental reports (e.g. Neitola et al., 2015; Rondo et al., 2016). Possible  
131 attachment of base and/or water molecules to single  $\text{H}_2\text{SO}_4$  molecules is not expected to have a  
132 notable effect on their detection efficiency. However, both free  $\text{H}_2\text{SO}_4$  molecules and those  
133 bound to base and/or water molecules are detected as single  $\text{H}_2\text{SO}_4$  molecules by CIMS, since  
134 the ligands are quickly lost upon the chemical ionization (e.g. Ortega et al., 2014). In this study  
135 the actual  $\text{H}_2\text{SO}_4$  concentrations are not of particular interest, we focus here only on relative loss  
136 of  $\text{H}_2\text{SO}_4$  along the flow tube. The concentration of sulfuric acid in gas phase was measured as  
137 97 m/z Da using CIMS along the flow tube (see Fig. 1) at the beginning (0 cm), in the middle  
138 (100 cm) and at the lower part in distances of 120, 140, 160, and 180 cm from the beginning and  
139 at the outlet (200 cm) of the flow tube in a wide range of relative humidities from 4 to 70 %. The  
140 CIMS sampling flow rate was set to  $71 \text{ min}^{-1}$ . In order to measure the  $\text{H}_2\text{SO}_4$  concentration along  
141 the whole flow tube, an additional CIMS inlet sampling tube was used - a stainless steel tube  
142 with I.D. 10 mm and whole length of 122 cm (100 cm straight + 22 cm elbow-pipe). The  
143 experimental measurement proceeded in the following way. First, all the experimental conditions  
144 (temperature of saturator and flow tube, flow rates, relative humidity) were adjusted. When the  
145 steady state was reached, the CIMS' inlet was connected to the lowest hole at 200 cm and  
146 concentration of sulfuric acid was recorded for at least 20 min. Afterwards the CIMS' inlet was  
147 moved up to the hole at 180 cm, and the same procedure was repeated until the last hole at the  
148 top of the tube was reached. To confirm the reproducibility of the experimental data the  $\text{H}_2\text{SO}_4$   
149 concentration at any arbitrary distance along the flow tube was measured again. Moreover, the  
150 reproducibility was checked by exchanging the flow tube parts, so that the part with 4 holes was



151 moved up, and  $\text{H}_2\text{SO}_4$  losses were measured in the distances 0, 20, 40, 60, 80, 100 and 200 cm,  
152 respectively.

153 **2.1 The CFD model**

154 To verify the assumption of laminar flow inside the tube, we applied the computational fluid  
155 dynamics model CFD-FLUENT (version 6.2) which simulates flow based on the Euler equations  
156 for mass and momentum conservation. These equations and the general operating principles of  
157 FLUENT are described in detail in Herrmann et al. (2006, 2009 and 2010). It has to be noted that  
158 unlike the earlier studies, this work did not include the Fine Particle Model (FPM). Particle  
159 production was thus not taken into account, and only sulfuric acid and water vapours are  
160 considered in the CFD-FLUENT simulations.

161 The simulations only considered the flow tube part of the experimental setup described in section  
162 2. Methods; the flow tube can be set up as an axisymmetric 2D problem. For the calculations  
163 presented here, we chose a resolution of  $50 \times 1000$  cells. The same geometry has been used in  
164 Herrmann et al. (2010). Boundary conditions (volumetric flow, wall temperatures, relative  
165 humidity, and initial sulfuric acid concentration) were set to match the experimental conditions.  
166 The wall was assumed to be an infinite sink for sulfuric acid, which means that the  $\text{H}_2\text{SO}_4$   
167 concentration at the walls was set to 0 in the simulations. Properties of sulfuric acid were  
168 identical to the ones described in our earlier work. Differing from Herrmann et al. (2010), there  
169 is no temperature gradient or buoyancy phenomena disturbing parabolic radial flow profile. To  
170 verify the proper operation of the setup we applied the diffusion coefficient derived  
171 experimentally in this work to FLUENT simulations. The simulations yielded a profile of  
172 sulfuric acid concentration inside the flow tube which we compared back to the experimental  
173 results.

174 **2.2 Experimental determination of the diffusion coefficient**

175 The wall loss of  $\text{H}_2\text{SO}_4$  in the flow tube was assumed to be a diffusion controlled first-order rate  
176 process, which can be described by a simple equation:

$$177 [\text{H}_2\text{SO}_4]_t = [\text{H}_2\text{SO}_4]_0 e^{-kt}, \quad (1)$$

178 where  $[\text{H}_2\text{SO}_4]_0$  is the initial concentration of  $\text{H}_2\text{SO}_4$ ,  $[\text{H}_2\text{SO}_4]_t$  is the concentration after time  $t$   
179 and  $k$  ( $\text{s}^{-1}$ ) is the rate constant, which is given by the equation:



180 
$$k = 3.65 \frac{D}{r^2}, \quad (2)$$

181 where  $r$  is the radius of the flow tube and  $D$  is the diffusion coefficient of  $\text{H}_2\text{SO}_4$ . Equation 2 is  
182 valid for diffusion in a cylindrical tube under laminar flow conditions and when the axial  
183 diffusion of the species investigated is negligible (Brown, 1978). The slopes obtained from linear  
184 fits to the experimental data  $\ln([\text{H}_2\text{SO}_4])$  as a function of the distance in the flow tube stand for  
185 the loss rate coefficient,  $k_{\text{obs}}$  ( $\text{cm}^{-1}$ ) assuming that the first order loss to the flow tube wall is the  
186 only sink for the gas phase  $\text{H}_2\text{SO}_4$ . Multiplying the loss rate coefficient  $k_{\text{obs}}$  with mean flow  
187 velocity in the flow tube ( $\text{cm s}^{-1}$ ) yields the experimental first-order wall loss rate coefficient  $k_w$   
188 ( $\text{s}^{-1}$ ), from which the diffusion coefficients of  $\text{H}_2\text{SO}_4$  were determined using Eq. 2. Hanson and  
189 Eisele (2000) reported that the wall of the flow tube can act as a source of  $\text{H}_2\text{SO}_4$  vapour after  
190 exposure in long lasting experiments and under very low relative humidity ( $\text{RH} \leq \sim 0.5\%$ ).  
191 The accuracy of our RH measurements is  $\pm 3\%$  RH, so to avoid any influence of  $\text{H}_2\text{SO}_4$   
192 evaporation from the flow tube wall we only used data measured at  $\text{RH} \geq 4\%$  in the final  
193 analysis. Furthermore, we performed CFD-FLUENT simulations at  $\text{RH}=5\%$  and  $T=298\text{ K}$ , with  
194 increased  $\text{H}_2\text{SO}_4$  concentration on the flow tube wall (0–100 % of  $[\text{H}_2\text{SO}_4]_0$ ), shown in Fig. 2.  
195 The comparison suggests that in our measurements the concentration on the flow tube wall is  
196 below 6 % of the  $[\text{H}_2\text{SO}_4]_0$  under all conditions. When the  $\text{H}_2\text{SO}_4$  concentration on the wall is  $\leq 6$   
197 % of  $[\text{H}_2\text{SO}_4]_0$ , the resulting difference in the obtained diffusion coefficient is within 10 % when  
198 compared to diffusion coefficient obtained with infinite sink boundary condition on the wall, as  
199 indicated by the shaded box in bottom left corner in Fig 2B. Any higher  $\text{H}_2\text{SO}_4$  concentration at  
200 the wall than 6 % of  $[\text{H}_2\text{SO}_4]_0$  would lead to a larger than 10 % decrease in the obtained diffusion  
201 coefficient.

### 202 **2.3 Quantum chemical data and cluster kinetics modeling**

203 To assess the effects of possible base impurities on the measurement results, we performed  
204 clustering kinetics simulations using quantum chemical input data for the stabilities of  $\text{H}_2\text{SO}_4$ –  
205 base clusters as described by Olenius et al. (2014). Since recent theoretical studies (e.g. Ortega et  
206 al., 2012; Kupiainen-Määttä et al., 2013; Loukonen et al. 2014) suggest and experiments (e.g.  
207 Zollner et al. 2012; Almeida et al. 2013; Kürten et al., 2014; Neitola et al., 2014, Rondo et al.  
208 2016) confirm that amines are more effective in stabilizing sulfuric acid clusters than ammonia,  
209 we focus only on the clustering of sulfuric acid with dimethylamine (DMA) and trimethylamine  
210 (TMA) and their hydrates (see also Section 3.2 Effect of Base Contaminants in Olenius et al.,



211 2014). The cluster kinetics approach does not consider the 2D flow profile, but only the central  
212 stream line of the flow, from which clusters and molecules are lost by diffusion. This is  
213 considered a reasonable assumption for a laminar flow, as also indicated by the CFD-FLUENT  
214 modeling results (see the Results section).

215 Detailed information on the simulations, as well as extensive discussion on the effects of  
216 clustering on the apparent diffusion coefficient can be found in the study by Olenius et al.  
217 (2014). Theoretical diffusion coefficients for sulfuric acid and representative base contaminant  
218 molecules and small acid–base clusters and their hydrates were calculated according to the  
219 kinetic gas theory. The effective diffusion coefficient corresponding to the experimental  
220 approach was determined by simulating the time evolution of the molecular cluster  
221 concentrations using cluster evaporation rates based on quantum chemical calculations at the  
222 B3LYP/CBSB7//RICC2/aug-cc-pV(T+d)Z level of theory, as described by Olenius et al. (2014).  
223 The simulations were run by setting initial concentrations for  $\text{H}_2\text{SO}_4$  and base monomers, and  
224 integrating the time development of the cluster concentrations for the experimental residence  
225 times. The initial acid concentration was set to be the average  $\text{H}_2\text{SO}_4$  monomer concentration  
226  $[\text{H}_2\text{SO}_4] = 5 \times 10^6 \text{ cm}^{-3}$  measured with CIMS at the beginning of the flow tube (see Fig. 1, hole 1)  
227 for all experimental conditions. For the initial base concentration we adopted a similar approach  
228 as described in Olenius et al. (2014): The initial base concentration was considered to be a)  
229 constant during the experiment, or b) RH dependent, i.e. base molecules enter the system with  
230 the water vapour; such a scenario seems to be reasonable since it was observed in several  
231 experimental set-ups (e.g. Benson et al., 2011; Brus et al., 2011; Kirkby et al., 2011). In the  
232 second case we set the initial base concentration  $[\text{base}]_{\text{init}}$  to be linearly proportional to RH as  
233

234  $[\text{base}]_{\text{init}} (\text{ppt}) = [\text{base}]_{\text{dry}} (\text{ppt}) + 0.1 \times \text{RH} (\%), \quad (3)$

235

236 where the linear relationship was based on a fit to DMA and TMA concentrations measured in  
237 the same experimental setup, but different experiments at various RH and  $\text{H}_2\text{SO}_4$  concentrations  
238 (Neitola et al., 2014 and 2015). The dry values  $[\text{base}]_{\text{dry}}$  were taken from Brus et al., (2016). The  
239 resulting initial base concentrations  $[\text{base}]_{\text{init}}$  for DMA and TMA were 4 and 2 ppt, respectively,  
240 at dry conditions (RH=0 %), and 10 and 8 ppt at RH=60 %. The simulations were performed for  
241 the three temperatures of 278, 288 and 298 K at atmospheric pressure (1 atm). The temperature  
242 dependency of the viscosity of the carrier gas, needed to calculate the diffusion coefficients of  
243 different species in the simulations (see Eq. (6) in Olenius et al., 2014), was taken to be



244 
$$\eta_{N_2} = \eta_{N_2,0} \left( \frac{T_0+C}{T+C} \right) \left( \frac{T}{T_0} \right)^{3/2}, \quad (4)$$

245 where  $\eta_{N_2,0} = 17.81 \times 10^{-6}$  Pa s,  $T_0 = 300.55$  K, and  $C = 111$  K (Crane Co., 1982).

### 246 3. Results and discussion

247 Figure 3 shows the diffusion coefficients of  $H_2SO_4$ , determined from the loss rate coefficients  $k_w$   
248 ( $s^{-1}$ ) using Eq. 2 as a function of RH at the three temperatures of 278, 288 and 298 K. The  
249 measured points are accompanied with the fit and  $H_2SO_4$  -  $N_2$  data at 298 K reported by Hanson  
250 and Eisele (2000). As can be seen, the diffusion coefficient values decreased as the RH was  
251 increased and the diffusion coefficient dependency on RH flattens in the range of RH 20-70 %.  
252 These results show lower wall losses and slower diffusion to the wall due to strong hydration of  
253  $H_2SO_4$  molecules (Jaeger-Voirol and Mirabel, 1988) and possibly  $H_2SO_4$  clustering with base  
254 impurities.

255 There are three previously reported experimental values of the  $H_2SO_4$  diffusion coefficient in  
256 nitrogen. Pöschl et al. (1998) reported a value of  $0.088 \text{ cm}^2 \text{ s}^{-1}$  at  $T=303$  K and  $\text{RH} \leq 3\%$ ,  
257 Lovejoy and Hanson (1996) reported a value of  $0.11 \text{ cm}^2 \text{ s}^{-1}$  at  $T=295$  K and  $\text{RH} \leq 1\%$ , and the  
258 study of Hanson and Eisele (2000) yielded a value of  $0.094 \text{ cm}^2 \text{ s}^{-1}$  at  $T=298$  K and  $\text{RH} \leq 1\%$ .  
259 The value of the diffusion coefficient of  $H_2SO_4$  in air at  $T=298$  K and  $\text{RH}=4\%$  determined in this  
260 study is  $0.08 \text{ cm}^2 \text{ s}^{-1}$ , which is in reasonable agreement with previously reported values, although  
261 the comparison is complicated because of slightly different experimental conditions and different  
262 carrier gases.

263 In Fig. 4 the  $H_2SO_4$  losses simulated with the CFD-FLUENT model described in section 2.1 are  
264 compared with experimental values, which were measured in a separate set of experiments  
265 conducted at  $T=278, 288$  and  $298$  K. The linear fit to the experimental data represents the loss  
266 rate coefficients ( $k_{\text{obs}}$ ,  $\text{cm}^{-1}$ ). As can be seen from Fig. 4, the model describes the behaviour of  
267  $H_2SO_4$  in the flow tube very well and confirms the validity of laminar flow approximation for all  
268 three temperatures. The maximum difference between the experimental and simulated values of  
269 the loss rate coefficient ( $k_{\text{obs}}$ ) was found 7 %, see Fig. 4D for details.

270 Semi-empirical predictions for binary diffusion coefficients can be calculated from the Fuller et  
271 al. equation which is based on fits to experimental data of various gases as described by Fuller et  
272 al. (1966) and Reid et al. (1987):

273

274 
$$D_{AB} = \frac{0.00143T^{1.75}}{P \sqrt{M_{AB}} \times \left[ \sqrt[3]{\left( \sum_v \right)_A} + \sqrt[3]{\left( \sum_v \right)_B} \right]^2}, \quad (4)$$



275

276 where  $D_{AB}$  is the binary diffusion coefficient of species A and B ( $\text{cm}^2 \text{ s}^{-1}$ ),  $T$  is the temperature  
277 (K),  $P$  is the pressure (bar),  $M_{AB}$  is  $2[(1/M_A) + (1/M_B)]^{-1}$  ( $\text{g mol}^{-1}$ ), where  $M_A$  and  $M_B$  are the  
278 molecular weights of species A and B ( $\text{g mol}^{-1}$ ), and  $\Sigma_i$  is calculated for each component by  
279 summing its atomic diffusion volumes (Reid et al., 1987). The functional form of Eq. (4) is  
280 based on the kinetic gas theory (the Chapman-Enskog theory), and the temperature dependence  
281 is obtained from a fit to a large set of experimental diffusion coefficients. A purely theoretical  
282 approach based on the kinetic gas theory with the hard-spheres approximation would yield a  
283 dependence of  $T^{1.5}$ . The calculated values of the diffusion coefficients of  $\text{H}_2\text{SO}_4$ , dimethylamine-  
284 and trimethylamine-sulfate in dry air at 298 K using the Fuller method are 0.11, 0.08 and 0.074  
285  $\text{cm}^2 \text{ s}^{-1}$ , respectively, which is in a reasonable agreement with our experimental data – the  
286 measured diffusion coefficient of  $\text{H}_2\text{SO}_4$  at  $T=298$  K under close to dry conditions (RH 4%) is  
287  $0.08 \text{ cm}^2 \text{ s}^{-1}$ . However, when calculating the diffusion coefficients of  $\text{H}_2\text{SO}_4$  in dry air at lower  
288 temperatures (278 and 288 K) with the Fuller method, the agreement of the experimental values  
289 with the predictions deteriorates. The formula predicts significantly higher diffusion coefficients  
290 than those observed in the experiments. The calculated values of  $D_{AB}$  for  $\text{H}_2\text{SO}_4$  are  $0.104 \text{ cm}^2 \text{ s}^{-1}$   
291 at  $T=288$  K and  $0.098 \text{ cm}^2 \text{ s}^{-1}$  at  $T=278$  K, and the measured values are  $0.07 \text{ cm}^2 \text{ s}^{-1}$  at ( $T=288$   
292 K and RH=8 %) and  $0.054 \text{ cm}^2 \text{ s}^{-1}$  at ( $T=278$  K and RH=16 %), respectively. The temperature  
293 dependency of the experimental diffusion coefficients was found to be a power of 5.4 for the  
294 whole dataset and temperature range. Since the data show a clear stepwise temperature  
295 dependency we provide also two separate fits to data from 278 to 288 K and from 288 to 298 K,  
296 with power dependencies of 2.2 and 8.7, respectively. These numbers are striking when  
297 compared to the empirical method of Fuller et al. (1966), who obtained the best fit to 340  
298 experimental diffusion coefficients with the power dependency of  $T \propto 1.75$ .

299 In Figure 5 we show the temperature dependency of the experimental data obtained from  
300 literature (Lovejoy and Hanson, 1996; Pöschl et al., 1998; Hanson and Eisele, 2000), predictions  
301 of the Fuller method for the diffusion coefficients of sulfuric acid, dimethylamine- and  
302 trimethylamine-sulfates in dry air, results of the clustering kinetics simulations using quantum  
303 chemical data for several simulated systems (discussed below), and the experimental data of this  
304 work. The data collected from literature, all obtained using laminar flow technique and  $\text{N}_2$  as the  
305 carrier gas, show a temperature dependency opposite to the one expected from theory. However,



306 the range of temperatures at which the measurements were carried out is quite narrow (only 8 K)  
307 and different experimental set-ups could explain such behaviour.  
308 The origin of the discrepancy in the temperature dependency of the diffusion coefficient in our  
309 experiment remains unclear; however, a possible explanation could be the increased clustering of  
310  $\text{H}_2\text{SO}_4$  at lower temperatures (see explanation below) with unavoidably present trace impurities  
311 in the system, such as amines. The CIMS was used to measure the concentrations of  $\text{H}_2\text{SO}_4$  gas  
312 phase monomers and dimers during the experiments; larger clusters were outside the mass range  
313 of the CIMS used. In order to explain the experimental observation of the temperature  
314 dependency of the diffusion coefficient, the dimer to monomer ratio at different temperatures  
315 was investigated. The  $\text{H}_2\text{SO}_4$  dimer formation is a result of  $\text{H}_2\text{SO}_4$  monomer collisions, and thus  
316 the observed  $\text{H}_2\text{SO}_4$  dimer CIMS signal depends on the  $\text{H}_2\text{SO}_4$  monomer concentration and also  
317 on the residence time, which determinates the time available for the clustering to take place  
318 (Petäjä et al., 2011). No significant temperature dependency of the [dimer]/[monomer] ratio was  
319 observed in our experiments, which is in agreement with Eisele and Hanson (2000), who report a  
320 relatively constant  $\text{H}_2\text{SO}_4$  [dimer]/[monomer] ratio with lowering temperature (the temperature  
321 range investigated in their study was 235 – 250 K). On the other hand, they report a substantial  
322 increase in the larger clusters' (trimer and tetramer) concentration with decreasing temperature  
323 while the monomer concentration was almost constant. There are only a very few previously  
324 reported values of the sulfuric acid dimer to monomer ratio from laboratory experiments. Petäjä  
325 et al. (2011) studied the close to collision-limited sulfuric acid dimer formation under  
326 experimental conditions similar to our study ( $T=293$  K, RH=22 %, initial  $\text{H}_2\text{SO}_4$  concentrations  
327 from  $10^6$  to  $10^8$  molecule  $\text{cm}^{-3}$  with saturator containing liquid  $\text{H}_2\text{SO}_4$  and in-situ  $\text{H}_2\text{SO}_4$  using  
328  $\text{O}_3$ -photolysis as methods for producing gas phase  $\text{H}_2\text{SO}_4$ ). They reported  $\text{H}_2\text{SO}_4$   
329 [dimer]/[monomer] ratios ranging from 0.05 to 0.1 at RH = 22 % and a residence time of 32 s.  
330 Petäjä et al. (2011) speculate about the presence of a third stabilizing compound, and their  
331 experimental dimer formation rates correspond well to modelled rates at a DMA concentration  
332 of about 5 ppt. Almeida et al. (2013) reported [dimer]/[monomer] ratios from 0.01 to 0.06 for the  
333 experiments in CLOUD chamber with addition of DMA (3-140 ppt, with the effect saturated for  
334 addition >5 ppt) and [dimer]/[monomer] ratios from  $1\times 10^{-4}$  to 0.003 for pure binary  $\text{H}_2\text{SO}_4$ -  
335 water system, both at RH=38 % and  $T=278$  K. In our measurements the  $\text{H}_2\text{SO}_4$   
336 [dimer]/[monomer] ratio under conditions  $T=298$  K, RH=24 % and a residence time of ~37 s,  
337 spans the range from 0.03 to 0.11, which is in reasonable agreement with values reported by both



338 Petäjä et al. (2011) and Almeida et al. (2013) when trace impurity levels of DMA are present in  
339 the system.

340 The cluster population simulations using quantum chemical data (see Figs. 5, 6 and Table 1)  
341 show that the presence of base impurities may decrease the effective  $\text{H}_2\text{SO}_4$  diffusion coefficient  
342 by attachment of base molecules to the acid. Simulations considering only hydrated  $\text{H}_2\text{SO}_4$   
343 molecules and no bases give higher values for the diffusion coefficient, and also a notably less  
344 steep temperature dependency (Table 1). Similarly to experiment the stepwise behaviour of  
345 temperature dependency could be found when fits are performed separately for temperatures  
346 278–288 K and 288–298 K, see Table 1. This demonstrates that temperature-dependent clustering  
347 may change the behaviour of the effective diffusion coefficient with respect to temperature.  
348 Results obtained by simulating clusters containing  $\text{H}_2\text{SO}_4$  and DMA are closer to the  
349 experimental diffusion coefficient values than those obtained using  $\text{H}_2\text{SO}_4$  and TMA. On the  
350 other hand, the power dependency shows a better agreement for the  $\text{H}_2\text{SO}_4$ –TMA system (see  
351 Table 1). The best agreement between the simulations and the experiment was found for the  
352 temperature 298 K. Also, changing the base concentration according to Eq. 3 shows a better  
353 performance than keeping the base concentration constant. Allowing the formation of clusters  
354 containing up to two  $\text{H}_2\text{SO}_4$  and two base molecules has no significant effect. In principle, the  
355 larger clusters bind  $\text{H}_2\text{SO}_4$  molecules and may thus increase the apparent diffusion coefficient,  
356 but here their effect is minor due to the relatively low initial  $\text{H}_2\text{SO}_4$  concentration of  $5 \times 10^6 \text{ cm}^{-3}$   
357 used in the simulations. More analysis on the effects of the amines can be found in the work by  
358 Olenius et al. (2014).

359 The formation of particles inside the flow tube during the experiments was measured regularly  
360 using Ultrafine Condensation Particle Counter (UCPC model 3776, TSI Inc. USA) with the  
361 lower detection limit of 3 nm. The highest determined concentration of particles was  
362 approximately  $2 \times 10^4$  yielding the maximum nucleation rate  $J$  of  $\sim 500 \text{ particles cm}^{-3} \text{ s}^{-1}$  at  
363  $T=278 \text{ K}$  and  $\text{RH}=60 \text{ \%}$ . Since the nucleation rate was increasing with decreasing temperature  
364 and elevated RH in the flow tube, the loss of gas phase sulfuric acid to the particles was more  
365 pronounced at temperatures of 288 and 278 K. The losses of  $\text{H}_2\text{SO}_4$  to particles were minimal –  
366 units of percent (see e.g. Brus et al. 2011 and Neitola et al. 2015 for details) and cannot explain  
367 our experimental observation of increased  $\text{H}_2\text{SO}_4$  diffusion coefficient temperature dependency.  
368 The additional losses of  $\text{H}_2\text{SO}_4$  would lead to increased values of observed loss rate coefficient  
369 ( $k_{\text{obs}}$ ) and subsequently to higher diffusion coefficient.



370 **4. Conclusions**

371 We have presented measurements of sulfuric acid diffusion coefficient in air derived from the  
372 first-order rate coefficients of wall loss of  $\text{H}_2\text{SO}_4$ . The experiments were performed in a laminar  
373 flow tube at temperatures 278, 288 and 298 K, relative humidities from 4 to 70 %, under  
374 atmospheric pressure and at initial  $\text{H}_2\text{SO}_4$  concentrations from  $10^6$  to  $10^8$  molec.  $\text{cm}^{-3}$ . The  
375 chemical ionization mass spectrometer (CIMS) was used to measure  $\text{H}_2\text{SO}_4$  gas phase  
376 concentration at seven different positions along the flow tube. The wall losses were determined  
377 from the linear fits to experimental  $\ln[\text{H}_2\text{SO}_4]$  as a function of axial distance in the flow tube.  
378 The losses of  $\text{H}_2\text{SO}_4$  inside the flow tube were also simulated using a computational fluid  
379 dynamics model (CFD-FLUENT), in which the wall is assumed to be an infinite sink for  $\text{H}_2\text{SO}_4$ .  
380 The experimentally determined  $\text{H}_2\text{SO}_4$  losses along the flow tube were in a very good agreement  
381 with profiles calculated using the FLUENT model, where experimentally obtained diffusion  
382 coefficients were used as an input. A maximum difference of ~7 % for experiments conducted at  
383  $T=278, 288$  and 298 K and in the whole RH range was found when compared to model. The  
384 results of the fluid dynamics model (CFD-FLUENT) also satisfactorily confirm the assumption of  
385 fully developed laminar profile inside the flow tube and infinite sink boundary conditions on the  
386 wall for  $\text{H}_2\text{SO}_4$  loss.

387 To explain an unexpectedly high power dependency of the  $\text{H}_2\text{SO}_4$  diffusion coefficient on  
388 temperature observed in our system we accounted in our calculations for involvement of base  
389 impurities: dimethyl- (DMA) and trimethyl-amine (TMA). The semi-empirical Fuller formula  
390 (Fuller et al., 1966) was used to calculate the diffusion coefficients at dry conditions for solely  
391  $\text{H}_2\text{SO}_4$ , and  $\text{H}_2\text{SO}_4$  neutralized with amine bases, namely dimethyamine- and trimethylamine-  
392 sulfate. Further, a molecular cluster kinetics model (Olenius et al. 2014) with quantum chemical  
393 input data was used to simulate acid–base cluster formation that may lead to the observed  
394 behaviour. With the simulations we obtained an effective diffusion coefficient determined in the  
395 same way as in the experiments.

396 The experimental  $\text{H}_2\text{SO}_4$  diffusion coefficients were found to be independent of different initial  
397  $[\text{H}_2\text{SO}_4]$  and a wide range of total flow rates. The values of the diffusion coefficient were found  
398 to decrease with increasing relative humidity owing to stronger hydration of  $\text{H}_2\text{SO}_4$  molecules.  
399 The observed power dependency of the experimental diffusion coefficients as a function of  
400 temperature was found to be of the order of 5.4 when the whole temperature range is accounted  
401 for which is in a clear disagreement with predictions from the Fuller method (Fuller et al., 1966)



402 having a power dependency of 1.75. Since the experimental diffusion coefficients deviate more  
403 from the theory towards the lower temperatures of 278 and 288 K, we suggest that a plausible  
404 explanation for this discrepancy is involvement of impurities such as amines, capable of binding  
405 to acid molecules with the binding strength increasing with decreasing temperature. This  
406 hypothesis is qualitatively supported by clustering kinetics simulations performed using quantum  
407 chemical input data for  $\text{H}_2\text{SO}_4$ –dimethylamine and  $\text{H}_2\text{SO}_4$ –trimethylamine clusters. Our results  
408 indicate that the effective diffusion coefficient of  $\text{H}_2\text{SO}_4$  in air exhibits a stronger temperature  
409 dependency than predicted from a theory that does not consider cluster formation, and neglecting  
410 this dependency might result in incorrect determination of residual  $\text{H}_2\text{SO}_4$  concentration in  
411 laboratory experiments. More measurements are therefore needed to gain a better understanding  
412 of the temperature dependency of the  $\text{H}_2\text{SO}_4$  diffusion coefficient and the formation of larger  
413  $\text{H}_2\text{SO}_4$  clusters.

414

#### 415 **Acknowledgement**

416 Authors would like to acknowledge KONE foundation, project CSF No. P209/11/1342, ERC  
417 project 257360-MOCAPAF, and the Academy of Finland Centre of Excellence (project number:  
418 272041) for their financial support.

419

420



421 **References**

422 Almeida, J., Schobesberger, S., Kürten, A., Ortega, I. K., Kupiainen-Määttä, O., Praplan, A. P.,  
423 Adamov, A., Amorim, A., Bianchi, F., Breitenlechner, M., David, A., Dommen, J., Donahue, N.  
424 M., Downard, A., Dunne, E. M., Duplissy, J., Ehrhart, S., Flagan, R. C., Franchin, A., Guida, R.,  
425 Hakala, J., Hansel, A., Heinritzi, M., Henschel, H., Jokinen, T., Junninen, H., Kajos, M.,  
426 Kangasluoma, J., Keskinen, H., Kupc, A., Kurtén, T., Kvashin, A. N., Laaksonen, A., Lehtipalo,  
427 K., Leiminger, M., Leppä, J., Loukonen, V., Makhmutov, V., Mathot, S., McGrath, M. J.,  
428 Nieminen, T., Olenius, T., Onnela, A., Petäjä, T., Riccobono, F., Riipinen, I., Rissanen, M.,  
429 Rondo, L., Ruuskanen, T., Santos, F. D., Sarnela, N., Schallhart, S., Schnitzhofer, R., Seinfeld, J.  
430 H., Simon, M., Sipilä, M., Stozhkov, Y., Stratmann, F., Tomé, A., Tröstl, J., Tsagkogeorgas, G.,  
431 Vaattovaara, P., Viisanen, Y., Virtanen, A., Vrtala, A., Wagner, P. E., Weingartner, E., Wex, H.,  
432 Williamson, C., Wimmer, D., Ye, P., Yli-Juuti, T., Carslaw, K. S., Kulmala, M., Curtius, J.,  
433 Baltensperger, U., Worsnop, D. R., Vehkamäki, H., and Kirkby, J.: Molecular understanding of  
434 sulphuric acid-amine particle nucleation in the atmosphere, *Nature*, 502, 359–363, 2013.  
435 Benson, D. R., Yu, J. H., Markovich, A., and Lee, S.-H.: Ternary homogeneous nucleation of  
436  $\text{H}_2\text{SO}_4$ ,  $\text{NH}_3$ , and  $\text{H}_2\text{O}$  under conditions relevant to the lower troposphere, *Atmos. Chem. Phys.*,  
437 11, 4755–4766, doi:10.5194/acp-11-4755-2011, 2011.  
438 Brown, R.L.: Tubular flow reactor with first-order kinetics, *J. Res. Natl. Bur. Stand. (U.S.)*, 83,  
439 1, 1-6, 1978.  
440 Brus, D., Neitola, K., Hyvärinen, A.-P., Petäjä, T., Vanhanen, J., Sipilä, M., Paasonen, P.,  
441 Kulmala, M., and Lihavainen, H.: Homogenous nucleation of sulfuric acid and water at close to  
442 atmospherically relevant conditions, *Atmos. Chem. Phys.*, 11, 5277– 5287, doi:10.5194/acp-11-  
443 5277-2011, 2011.  
444 Brus, D., Hyvärinen, A.-P., Anttila, T., Neitola, K., Merikanto, J., Duplissy, J., Koskinen, J.,  
445 Makkonen, U., Hellén, H., Hemmilä, M., Sipilä, M., Mauldin III, R. L., Jokinen, T., Petäjä, T.,  
446 Kurtén, T., Vehkamäki, H., Kulmala, M., Viisanen, Y., Lihavainen, H., and Laaksonen, A.: On  
447 sulphuric acid saturation vapour pressure: insight into measurements and implementation of  
448 results, *J. Geophys. Res. Atmospheres*, submitted, 2016.  
449 Crane Co. and Crane Co. Engineering Division: Flow of Fluids Through Valves, Fittings, and  
450 Pipe, Crane Company, Technical paper, 1982.



451 Eisele, F. L., and Tanner, D.: Measurement of the gas phase concentration of  $\text{H}_2\text{SO}_4$  and  
452 methane sulphonic acid and estimates of  $\text{H}_2\text{SO}_4$  production and loss in the atmosphere, *J.*  
453 *Geophys. Res.*, 98, 9001–9010, 1993.

454 Eisele, F. L., and Hanson D. R.: First measurement of prenucleation molecular clusters, *J. Phys.*  
455 *Chem. A*, 104(4), 830–836, doi:10.1021/jp9930651, 2000.

456 Fuller, E. N., Schettler, P. D., and Giddings, J. C.: New method for prediction of binary gas-  
457 phase diffusion coefficients, *Ind. Eng. Chem.*, 58, 18–27, 1966.

458 Hanson, D. R. and Eisele, F. L.: Diffusion of  $\text{H}_2\text{SO}_4$  in humidified nitrogen: Hydrated  $\text{H}_2\text{SO}_4$ , *J.*  
459 *Phys. Chem. A*, 104, 1715–1719, 2000.

460 Herrmann, E., Lihavainen, H., Hyvärinen, A. P., Riipinen, I., Wilck, M., Stratmann, F. and  
461 Kulmala, M.: Nucleation simulations using the fluid dynamics software FLUENT with the fine  
462 particle model FPM, *J. Phys. Chem. A*, 110, 12448–12455, 2006.

463 Herrmann, E., Hyvärinen, A. P., Brus, D., Lihavainen, H. and Kulmala, M.: Re-evaluation of the  
464 pressure effect for nucleation in laminar flow diffusion chamber experiments with fluent and the  
465 fine particle model, *J. Phys. Chem. A*, 113, 1434–1439, 2009.

466 Herrmann, E., Brus, D., Hyvärinen, A.-P., Stratmann, F., Wilck, M., Lihavainen, H. and  
467 Kulmala, M.: A computational fluid dynamics approach to nucleation in the water-sulphuric acid  
468 system, *J. Phys. Chem. A*, 114, 8033–8042, 2010.

469 Jaecker-Voirol, A. and Mirabel, P.: Nucleation rate in binary mixture of sulphuric acid-water  
470 vapour: A re-examination, *J. Phys. Chem.*, 92(12), 3518–3521, 1988.

471 Kirkby, J., Curtius, J., Almeida, J., Dunne, E., Duplissy, J., Ehrhart, S., Franchin, A., Gagné, S.,  
472 Ickes, L., Kürten, A., Kupc, A., Metzger, A., Riccobono, F., Rondo, L., Schobesberger, S.,  
473 Tsagkogeorgas, G., Wimmer, D., Amorim, A., Bianchi, F., Breitenlechner, M., David, A.,  
474 Dommen, J., Downard, A., Ehn, M., Flagan, R., Haider, S., Hansel, A., Hauser, D., Jud, W.,  
475 Junninen, H., Kreissl, F., Kvashin, A., Laaksonen, A., Lehtipalo, K., Lima, J., Lovejoy, E.,  
476 Makhmutov, V., Mathot, S., Mikkilä, J., Minginette, P., Mogo, S., Nieminen, T., Onnela, A.,  
477 Pereira, P., Petäjä, T., Schnitzhofer, R., Seinfeld, J., Sipilä, M., Stozhkov, Y., Stratmann, F.,  
478 Tomé, A., Vanhanen, J., Viisanen, Y., Aron Vrtala, A., Wagner, P., Walther, H., Weingartner,  
479 E., Wex, H., Winkler, P., Carslaw, K., Worsnop, D., Baltensperger, U., and Kulmala, M.: Role



480 of sulphuric acid, ammonia and galactic cosmic rays in atmospheric aerosol nucleation, *Nature*,  
481 476, 429–433, doi:10.1038/nature10343, 2011

482 Kupiainen-Määttä, O., Olenius T., Kurtén T., and Vehkamäki H.: CIMS Sulfuric Acid Detection  
483 Efficiency Enhanced by Amines Due to Higher Dipole Moments: A Computational Study, *J.*  
484 *Phys. Chem. A*, 117(51), 14109–14119, doi:10.1021/jp4049764, 2013.

485 Kürten, A., Jokinen, T., Simon, M., Sipilä, M., Sarnela, N., Junninen, H., Adamov, A., Almeida,  
486 J., Amorim, A., Bianchi, F., Breitenlechner, M., Dommen, J., Donahue, N. M., Duplissy, J.,  
487 Ehrhart, S., Flagan, R. C., Franchin, A., Hakala, J., Hansel, A., Heinritzi, M., Hutterli, M.,  
488 Kangasluoma, J., Kirkby, J., Laaksonen, A., Lehtipalo, K., Leiminger, M., Makhmutov, V.,  
489 Mathot, S., Onnela, A., Petäjä, T., Praplan, A. P., Riccobono, F., Rissanen, M. P., Rondo, L.,  
490 Schobesberger, S., Seinfeld, J. H., Steiner, G., Tomé, A., Tröstl, J., Winkler, P. M., Williamson,  
491 C., Wimmer, D., Ye, P., Baltensperger, U., Carslaw, K. S., Kulmala, M., Worsnop, D. R., and  
492 Curtius, J.: Neutral molecular cluster formation of sulfuric acid-dimethylamine observed in real-  
493 time under atmospheric conditions, *Proc. Natl. Acad. Sci.*, 111(42), 15019–15024,  
494 doi:10.1073/pnas.1404853111, 2014.

495 Loukonen, V., Kuo, I.-F. W., McGrath, M. J., and Vehkamäki, H.: On the stability and dynamics  
496 of (sulfuric acid) (ammonia) and (sulfuric acid) (dimethylamine) clusters: A first-principles  
497 molecular dynamics investigation, *Chem. Phys.*, 428, 164–174,  
498 doi:10.1016/j.chemphys.2013.11.014, 2014.

499 Lovejoy, E. R. and Hanson, D. R.: Kinetics and products of the reaction  $\text{SO}_3 + \text{NH}_3 + \text{N}_2$ , *J.*  
500 *Phys. Chem.*, 100, 4459–4465, 1996.

501 Marti, J.J., Jefferson, A., Cai, X. P., Richert, C., McMurry, P. H. and Eisele, F.: The  $\text{H}_2\text{SO}_4$   
502 vapor pressure above sulphuric acid and ammonium sulphate solutions, *J. Geophysical Res.*,  
503 102(D3) 3725–3735, 1997.

504 Mauldin III, R.L., Frost, G., Chen, G., Tanner, D., Prevot, A., Davis, D., and Eisele, F.: OH  
505 measurements during the First Aerosol Characterization Experiment (ACE 1): Observations and  
506 model comparisons, *J. Geophys. Res.*, 103, 16713–16729, 1998.

507 Neitola, K., Brus, D., Makkonen, U., Sipilä, M., Lihavainen, H. and Kulmala, M.: Effect of  
508 addition of four base compounds on sulphuric-acid–water new-particle formation: a laboratory  
509 study, *Boreal Env. Res.* 19 (suppl. B): 257–274, 2014.



510 Neitola, K., Brus, D., Makkonen, U., Sipilä, M., Mauldin III, R. L., Sarnela, N., Jokinen, T.,  
511 Lihavainen, H., and Kulmala, M.: Total sulfate vs. sulfuric acid monomer concentrations in  
512 nucleation studies, *Atmos. Chem. Phys.*, 15, 3429-3443, doi:10.5194/acp-15-3429-2015, 2015

513 Olenius, T., Kurtén, T., Kupiainen-Määttä, O., Henschel, H., Ortega, I. K., Vehkamäki, H.:  
514 Effect of Hydration and Base Contaminants on Sulfuric Acid Diffusion Measurement: A  
515 Computational Study, *Aerosol Sci. and Tech.*, 48:6, 593-603, doi:  
516 10.1080/02786826.2014.903556, 2014.

517 Ortega, I., Olenius, T., Kupiainen-Määttä, O., Loukonen, V., Kurtén, T., and Vehkamäki, H.:  
518 Electrical charging changes the composition of sulfuric acid–ammonia/dimethylamine clusters,  
519 *Atmos. Chem. Phys.*, 14(15), 7995-8007, doi: 10.5194/acp-14-7995-2014, 2014.

520 Petäjä, T., Mauldin, III, R. L., Kosciuch, E., McGrath, J., Nieminen, T., Paasonen, P., Boy, M.,  
521 Adamov, A., Kotiaho, T., and Kulmala, M.: Sulphuric acid and OH concentrations in a boreal  
522 forest site, *Atmos. Chem. Phys.*, 9, 7435-7448, doi:10.5194/acp-9-7435-2009, 2009.

523 Petäjä, T., Sipilä, M., Paasonen, P., Nieminen, T., Kurtén, T., Ortega, I. K., Stratmann, F., Hanna  
524 Vehkamäki, H., Berndt, T. and Kulmala M.: Experimental Observation of Strongly Bound  
525 Dimers of Sulphuric Acid: Application to Nucleation in the Atmosphere, *Phys. Rev. Lett.*, 106,  
526 228302, 2011.

527 Pöschl, U., Canagaratna, M., Jayne, J.T., Molina, L.T., Worsnop, D.R., Kolb, C.E., Molina,  
528 M.J.: Mass accommodation coefficient of  $H_2SO_4$  vapor on aqueous sulphuric acid surfaces and  
529 gaseous diffusion coefficient of  $H_2SO_4$  in  $N_2/H_2O$ , *Journal of Physical Chemistry A*, 102, 10082-  
530 10089, 1998.

531 Reid, R. C., Prausnitz, J. M. and Polling B. E.: The properties of gases and liquids, fourth  
532 edition, Mc Graw-Hill Inc, New York, 1987.

533 Rondo, L., S. Ehrhart, A. Kürten, A. Adamov, F. Bianchi, M. Breitenlechner, J. Duplissy, A.  
534 Franchin, J. Dommen, N. M. Donahue, E. M. Dunne, R. C. Flagan, J. Hakala, A. Hansel, H.  
535 Keskinen, J. Kim, T. Jokinen, K. Lehtipalo, M. Leiminger, A. Praplan, F. Riccobono, M. P.  
536 Rissanen, N. Sarnela, S. Schobesberger, M. Simon, M. Sipilä, J. N. Smith, A. Tomé, J. Tröstl, G.  
537 Tsagkogeorgas, P. Vaattovaara, P. M. Winkler, C. Williamson, U. Baltensperger, J. Kirkby, M.  
538 Kulmala, D. R. Worsnop, and J. Curtius: Effect of dimethylamine on the gas phase sulfuric acid  
539 concentration measured by Chemical Ionization Mass Spectrometry (CIMS). *J. Geophys. Res.*  
540 *Atmos.*, 120, doi: 10.1002/2015JD023868, 2016.



541 Seinfeld, J. H. and Pandis, S. N.: *Atmospheric Chemistry and Physics: From Air Pollution to*  
542 *Climate Change*, John Wiley, New York, 1998.

543 Skrabalova, L., Brus, D., Antilla, T., Zdimal, V. and Lihavainen, H.: Growth of sulphuric acid  
544 nanoparticles under wet and dry conditions, *Atmos. Chem. Phys.*, 14, 1-15, 2014.

545 Tang, M. J., Cox, R. A., and Kalberer, M.: Compilation and evaluation of gas phase diffusion  
546 coefficients of reactive trace gases in the atmosphere: volume 1. Inorganic compounds, *Atmos.*  
547 *Chem. Phys.*, 14, 9233-9247, doi:10.5194/acp-14-9233-2014, 2014

548 Zollner, J. H., Glasoe, W. A., Panta, B., Carlson, K. K., McMurry, P. H., and Hanson, D. R.:  
549 Sulfuric acid nucleation: power dependencies, variation with relative humidity, and effect of  
550 bases, *Atmos. Chem. Phys.*, 12, 4399–4411, doi:10.5194/acp-12-4399- 2012, 2012.

551



552 **Table 1.** Summary of simulated and experimental averages (unweighted over RH) of the  
553 effective  $\text{H}_2\text{SO}_4$  diffusion coefficients  $D$  ( $\text{cm}^2 \text{ s}^{-1}$ ) with standard deviations in parenthesis for  
554 three temperatures 278, 288 and 298 K. The initial base concentration  $[\text{base}]_{\text{init}}$  is set to be either  
555 RH-dependent according to Eq. (3) or RH-independent, and the simulations consider clusters  
556 containing up to one acid and one base molecule (“1×1”) or two acid and two base molecules  
557 (“2×2”) as well as hydrates of the clusters. Power dependencies with respect to the temperature,  
558 obtained as linear fits to the data, are also listed.

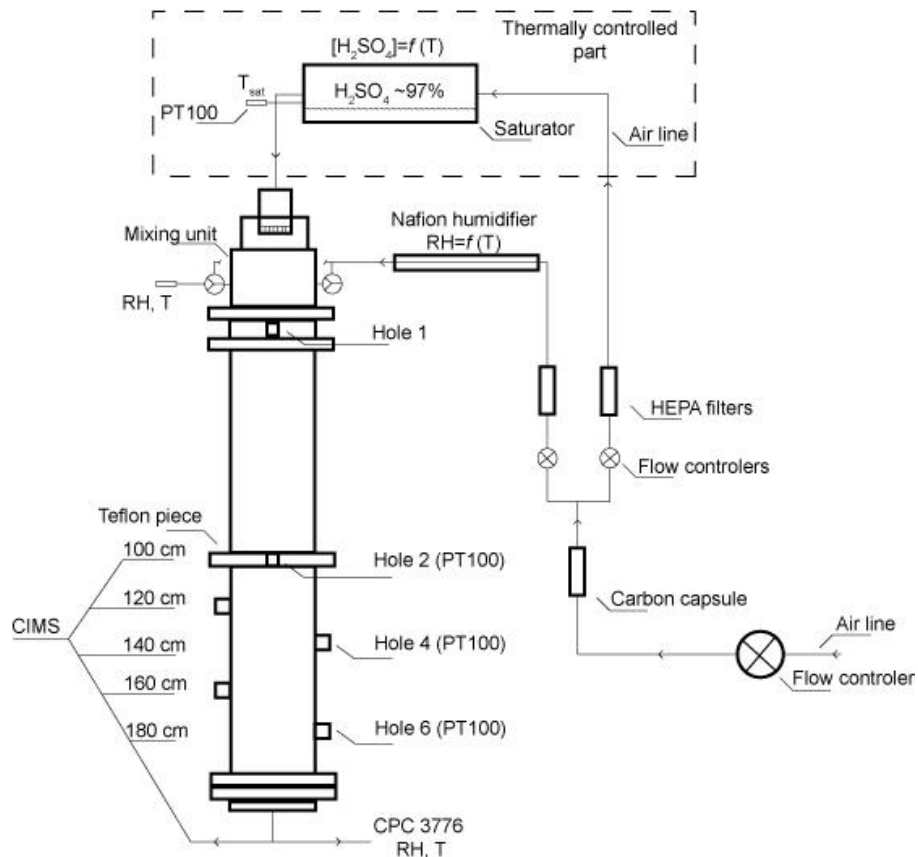
559

Impurities			$D$ ( $T=278\text{K}$ )	$D$ ( $T=288\text{K}$ )	$D$ ( $T=298\text{K}$ )	Power dependency*	
Base	$[\text{Base}]_{\text{init}}$	Simulated clusters					
DMA	(0.1xRH+4) ppt	1x1	0.064 (7%)	0.069 (7%)	0.077 (7%)	2.20/3.18/2.68	
		2x2	0.067 (6%)	0.072 (6%)	0.079 (6%)	2.06/2.92/2.48	
	Constant 5 ppt	1x1	0.067 (4%)	0.072 (4%)	0.080 (4%)	2.16/3.01/2.58	
		2x2	0.069 (3%)	0.074 (4%)	0.081 (4%)	2.02/2.77/2.39	
TMA	(0.1xRH+2) ppt	1x1	0.065 (7%)	0.071 (6%)	0.080 (4%)	2.40/3.53/2.95	
		2x2	0.068 (6%)	0.073 (5%)	0.081 (4%)	2.16/3.04/2.59	
	Constant 2 ppt	1x1	0.065 (2%)	0.071 (2%)	0.080 (1%)	2.41/3.52/2.95	
		2x2	0.067 (2%)	0.073 (2%)	0.081 (1%)	2.15/3.04/2.58	
Only SA hydrates			0.079 (4%)	0.084 (4%)	0.089 (4%)	1.67/1.67/1.67	
Experiment, this work			0.051 (11%)	0.055 (11%)	0.074 (7%)	2.18/8.70/5.35	

560 \*power dependency given separately for the temperature ranges 278-288 K / 288-298 K / the  
561 whole dataset temperature range (278-298 K), the same RH range is used for both simulations  
562 and experiment.



563



564

565

566 Figure 1. The schematic figure of the FMI flow tube.

567

568

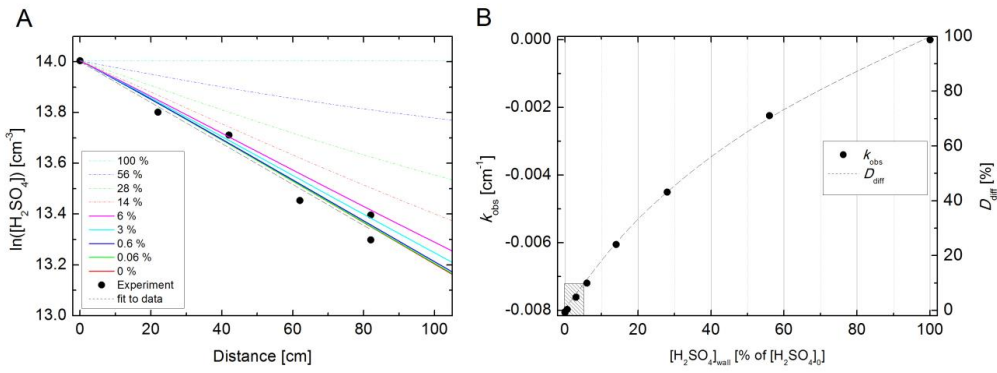
569

570

571

572

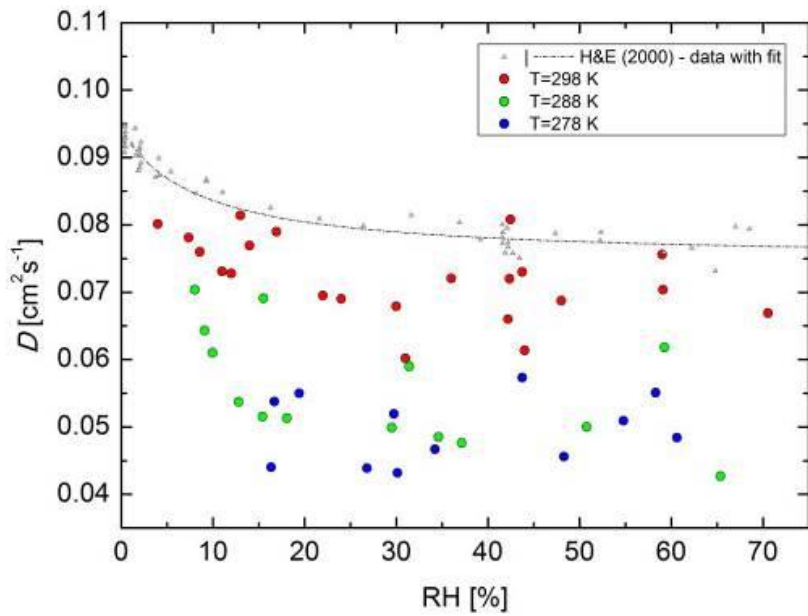
573



574

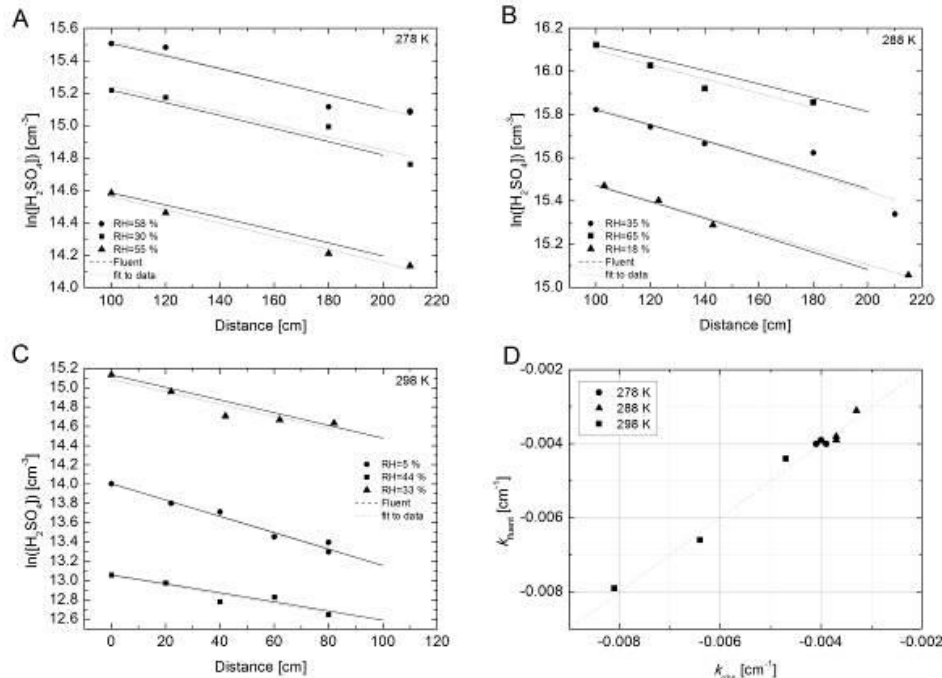
575 Figure 2. CFD-FLUENT simulations of influence of increased  $H_2SO_4$  concentration on the flow  
576 tube wall. A)  $\ln[H_2SO_4]$  as function of distance in the flow tube. B)  $k_{obs}$  and diffusion coefficient  
577 difference from the infinite sink boundary condition ( $D_{diff}$ ) as a function of the  $H_2SO_4$  wall  
578 concentration expressed as % of initial  $H_2SO_4$  concentration,  $[H_2SO_4]_0$ . The simulations  
579 conditions were RH=5 %,  $T=298$  K and  $Q_{tot}=7.6$  lpm. When the  $H_2SO_4$  concentration on the  
580 wall is  $\leq 6$  % of  $[H_2SO_4]_0$ , the resulting difference in the obtained diffusion coefficient is within  
581 10 % when compared to diffusion coefficient obtained with infinite sink boundary condition on  
582 the wall, as indicated by the shaded box in bottom left corner in Fig 2B.

583



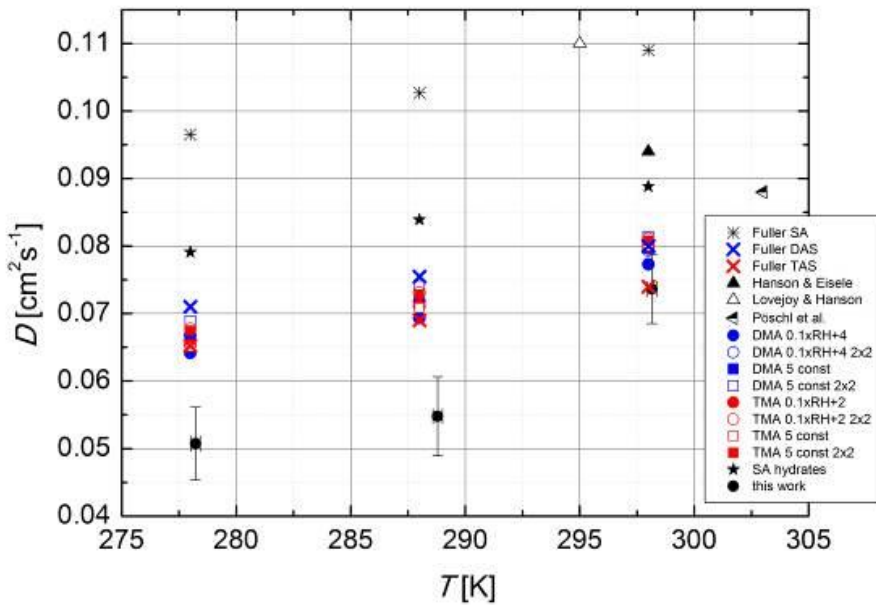
584

585 Figure 3. Experimental diffusion coefficient of  $\text{H}_2\text{SO}_4$  in air as a function of relative humidity at  
586 different temperatures compared with fit to the  $\text{H}_2\text{SO}_4$  diffusion in  $\text{N}_2$  data of Hanson and Eisele  
587 (2000).



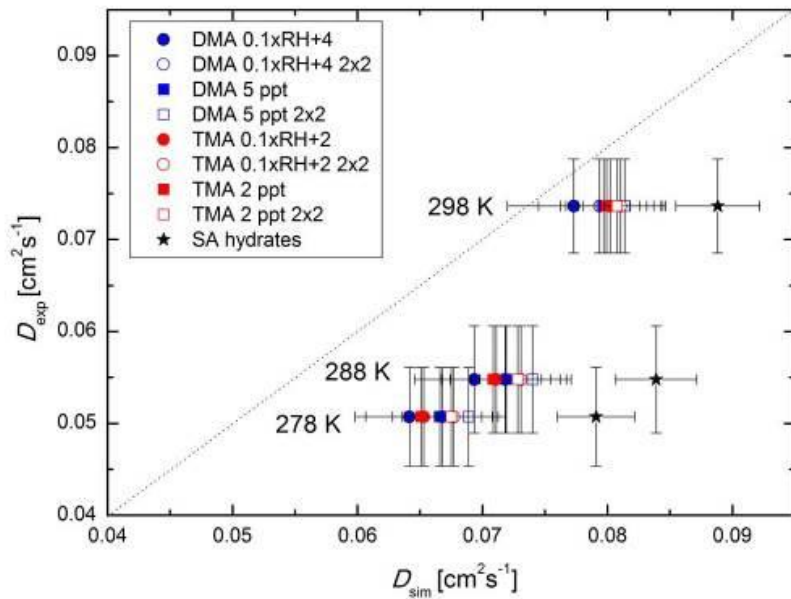
588

589 Figure 4. The sulfuric acid losses simulated with CFD-FLUENT model when the experimentally  
 590 obtained diffusion coefficients are used as an input at A)  $T=278$  K B)  $T=288$  K and C)  $T= 298$  K.  
 591 D) simulated losses rate coefficients compared with experimental values of  $k_{\text{obs}}$  (cm<sup>-1</sup>) at  $T=278$ ,  
 592 288 and 298 K.



593

594 Figure 5. The temperature dependency of the effective  $\text{H}_2\text{SO}_4$  diffusion coefficient, calculated  
595 using the Fuller method for dry  $\text{H}_2\text{SO}_4$  (SA), dimethylamine- (DAS) and trimethylamine-sulfate  
596 (TAS), both in dry air, data from literature, several assemblies of cluster population simulations  
597 (see text for details) and data measured experimentally in this work. The temperature  
598 dependency of the experimental diffusion coefficients was found to be a power of 6.  
599



600

601 Figure 6. Comparison of the experiment and the cluster population simulations at different  
602 temperatures, considered are also different levels and sources of impurities in the system. The  
603 formation of clusters containing up to two  $\text{H}_2\text{SO}_4$  and two base molecules is denoted as “2×2” in  
604 the legend.

605